Structure of Cu(115): Clean surface and its oxygen-induced facets

D. A. Walko* and I. K. Robinson
Department of Physics, University of Illinois at Urbana-Champaign, 1110 West Green Street, Urbana, Illinois 61801
(Received 21 January 1999)

Cu(001) vicinal surfaces facet when exposed to O. We have studied this process on Cu(115), which transforms from a clean surface to {104} and {113} facets, using surface x-ray diffraction. The Cu(115) surface exhibits a complex interlayer relaxation accounted for by basic elasticity theory; the vertical displacements of the three surface atoms are found to correlate with those of the subsurface atoms directly below. The O/Cu(104) facets do not, as previously proposed, involve any missing Cu rows, but the top three rows are expanded away from the bulk; the Cu-O chains which stabilize this surface are similar to those present on other O on Cu reconstructions. The O/Cu(113)(3×1) facets are significantly disordered, with stripes about 8 Å wide running parallel to the atomic steps. [S0163-1829(99)01224-2]

I. INTRODUCTION

The structures of many crystalline surfaces are affected by the adsorption of foreign species,[1] sometimes undergoing minor rearrangements to accommodate the adsorbed atoms or molecules, in other situations undergoing major transformations. Some adsorbed species induce highly organized reconstructions, while others form incommensurate overlayers. Yet others can destroy the inherent reconstructions formed on clean surfaces, such as the well-known case of H on Si$(001)(2\times1)$.[2] In other cases, surface adsorbates lead not to additional order, but to disorder such as surface alloying (exhibited in certain metal-on-metal systems),[3] surface roughening, or even amorphization. Under appropriate circumstances, faceting, the breaking up of a flat surface into large-scale terraces with particular crystallographic orientations, can occur. Whether the driving force is primarily short-range chemical forces, a longer-ranged charge-density wave,[4] or surface stress reduction,[5] the system attempts to reach an equilibrium state which minimizes the surface free energy.

Here we report on structures formed by the influence of oxygen on high-Miller-index copper surfaces. The reconstructions formed by O on low-index Cu are already well known, and were reviewed in Ref. 6. On Cu(110), O forms a 2×1 reconstruction[7] at low coverage and a $c(6\times2)$ reconstruction at higher coverage.[8] On Cu(001), O induces only a $2\sqrt{2}\times\sqrt{2}$ reconstruction[9] (although other superstructures had preliminarily been reported as discussed in Ref. 9). A common structural feature of these reconstructions[10] is the formation of Cu-O chains on these surfaces. The O atoms are fourfold coordinated, with all O-Cu bond lengths about 1.85 Å . These features are conspicuously similar to the characteristics of bulk cuprite, Cu_2O, except the O atoms of these reconstructions are not centered in Cu tetrahedra.[10] O on Cu(111) induces a more complex series of reconstructions which are rotated relative to the substrate, yet are comparable with the structure of bulk $Cu_2O(111)$ planes.[11,12] Recent studies of O/Cu$(102)(2\times1)$ have also found evidence for Cu-O-Cu chains on this surface, although that structure has not been fully determined.[13,14] Similar structures have also been found in the oxidation of Cu alloy surfaces[15,16] and Cu thin films.[17] One notable exception is that of O/Cu(112), which forms several reconstructions depending on experimental conditions, none of which have the Cu-O-Cu chain feature.[18]

Unlike these low-index surfaces, most high-index Cu surfaces do not form stable reconstructions, but rather facet when exposed to oxygen. Most Cu(001) vicinal surfaces form O/Cu(104) facets.[19–27] Of course, to maintain the surface's macroscopic orientation, other facets must form across the surface as well, such as {001} for the faceting of Cu(106) (Ref. 27) and Cu(108).[25] In this report we discuss the O-induced faceting of Cu(115), in the temperature range $200-400\,^{\circ}\mathrm{C}$, which forms facets with (104), (014), and (113) orientations. Since they are crystallographically equivalent, we implicitly include the O/Cu(014) facets in the following discussions of O/Cu(104) unless stated otherwise. This paper describes the surface structure of these facets as well as that of the clean Cu(115) surface. Elsewhere,[28,29] we described the kinetics of the faceting process as observed by x-ray diffraction.

Before moving on to the crystallographic structure of the clean and faceted surfaces, we comment on the ability to observe facet structures using surface x-ray diffraction. Crystal truncation rods (CTR's) occur because a surface breaks the periodicity of a bulk crystal.[30] A facet is a small area of the surface with a particular crystallographic orientation which does not correspond to that of the macroscopic surface. Yet it is still a surface, and the intensity of a CTR can be calculated in the usual way[30]:

$$I\propto\left|\sum_{n=-\infty}^{0}F\exp(-in\mathbf{q}\cdot\mathbf{c})\right|^2\propto|F|^2\frac{1}{4\sin^2(\mathbf{q}\cdot\mathbf{c}/2)}. \quad (1)$$

When applying Eq. (1) to a facet, the unit cell is chosen such that the lattice parameter c is perpendicular to the facet plane (instead of the bulk surface plane, as is the case for an unfaceted surface). The scattered intensity from one single facet will be small, proportional to the area of the facet. But if many facets of a given orientation are present on a surface, the scattering from their CTR's will add incoherently and the intensities become large enough to be observed.

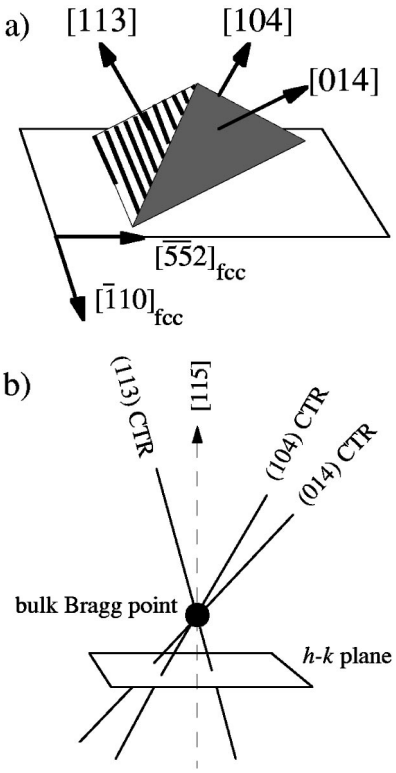

FIG. 1. (a) Schematic real-space model of one faceted pyramid, as observed with STM in Ref. 26. The surface normals of the (104), (014), and (113) facets are shown. The vertical scale is significantly exaggerated. (b) Schematic reciprocal-space diagram of CTR's due to the three facets in a). The $l=$const plane below the bulk Bragg peak is the plane of Fig. 2(b).

The scanning tunneling microscopy (STM) images of Reiter and Taglauer[26] show that the facets formed by exposing Cu(115) to O produce three-sided pyramids across the surface; each side is (at least) moderately well-ordered with well-defined orientations of (104), (014), or (113). One such pyramid is diagrammed in Fig. 1(a). The three facets are clearly distinguishable in the original micrograph,[26] as are the high degree of atomic ordering on the {104} facets and the relative disorder on the (113) facets.

We have observed CTR's from these three facets with surface x-ray diffraction, as demonstrated in Fig. 2. Figure 2(a) is a cross section through reciprocal space at constant perpendicular momentum transfer $l=\mathbf{q}\cdot\mathbf{c}$. The plane is thus parallel to the (115) surface with l (in this case) slightly greater than that of the bulk Bragg peak. This surface was prepared by exposing Cu(115) at 300 °C to ~20-L O_2 (1 L = 1 Langmuir = 10^{-6} Torr sec). No longer is this surface (115) oriented; if it were, a CTR would pass through the center of this plot at $h=6$ and $k=0$ (see below). Instead, the plot cuts through three rods, all of which are angled toward the bulk peak and perpendicular to the plane of their particular facet. On the lower side of the Bragg peak, the peaks have reversed positions, as shown in Fig. 2(b). Figure 1(b) depicts the constant-l plane cutting through the three CTR's, where l is less than that of the bulk peak. The well-defined orientations of the facets permit structure factors to be measured along the rods of each facet; the crystallographic analyses of these facets are in Secs. III and IV below.

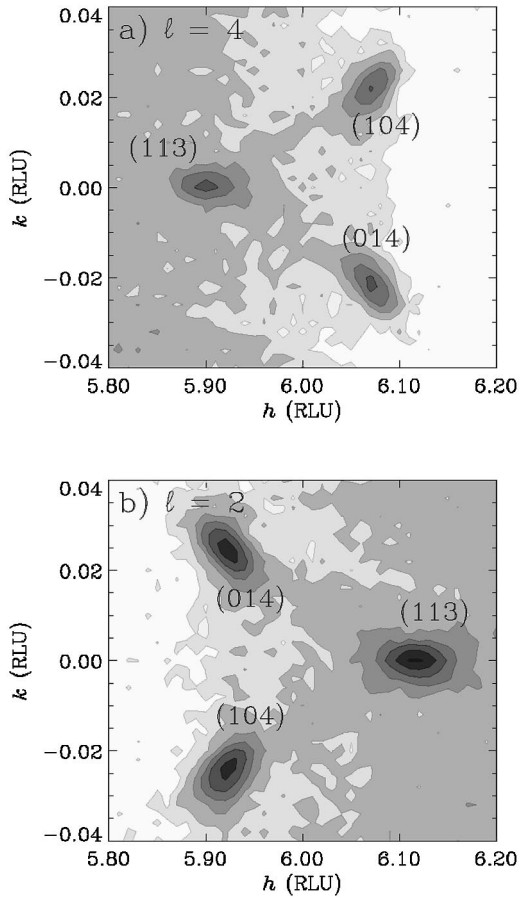

FIG. 2. (a) A cross section through reciprocal space above the $(603)_{115}$ bulk point, at $l=4$. The three spots are located at the intersection of the $l=4$ plane and the CTR's of the three facets formed by exposing O to Cu(115), as labeled. No (115) rod is visible at $h=6$ and $k=0$, indicating the surface is entirely faceted. (b) The same mesh scan, but now below the Bragg peak, at $l=2$. Each spot is now on the reverse side of the (115) CTR position.

In labeling the axes for the bulk surface and the two facets discussed in this paper, we follow standard surface science practice of labeling the surface normal as the z axis. In the surface plane, we choose y parallel to the steps on these vicinal surfaces, and $+x$ pointing toward an upward step. Thus our choice of coordinate system changes for each surface. The coordinates x, y, and z are given in units of the appropriate surface unit cell.

II. CLEAN CU(115) SURFACE STRUCTURE

Ideal Cu(115) is a regularly stepped vicinal surface of Cu(001). Compact step notation[31] describes its structure as $3(001)\times(111)$, meaning the surface is composed of {001} terraces (three atoms long) separated by ⟨111⟩-type (closed-packed) steps along the y direction. The angle between the [115] and [001] directions is 15.8°. Figure 3 illustrates the bulk-terminated Cu(115) surface, highlighting the three inequivalent atomic sites on the surface,[32] which all have different coordination numbers. Atoms on the step sites (S in Fig. 3) have seven nearest neighbors, while atoms at the terrace sites (T) have eight, and atoms at the corner sites (C) have ten. All other atoms are in fully coordinated ''bulklike''

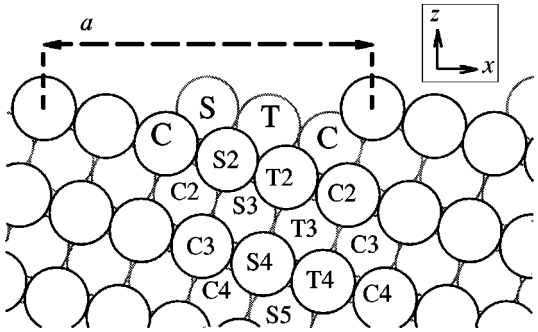

FIG. 3. Bulk-truncated structure of a clean, ideal fcc(115) surface. z is the surface normal, x runs perpendicular to the steps in the surface plane, and y is parallel to the surface steps (and perpendicular to the page). The surface atoms thus have small vertical separations, accounting for the small interlayer spacing ($d_{bulk}=0.696$ Å). Atoms at the surface are labeled according to their location at the step (S), on the terrace (T), or at the corner below the next step (C) (Refs. 32 and 37). Subsurface atoms are labeled according to the surface atom above them and their depth (in atoms) below the surface (along the column of similar atoms).

sites. In the centered orthorhombic surface unit cell, each atom at (x,y,z) has a crystallographically equivalent atom at $(x+\frac{1}{2},y+\frac{1}{2},z)$, in units of the surface unit cell.

Because of the high Miller indices of this surface, the reciprocal space notation is rather complicated. The geometric transformations between standard fcc coordinates and (115) surface coordinates are given by the following matrices:

$$\begin{pmatrix} h \\ k \\ l \end{pmatrix}_{(115)} = \begin{pmatrix} \frac{5}{2} & \frac{5}{2} & 1 \\ -\frac{1}{2} & \frac{1}{2} & 0 \\ -1 & -1 & 5 \end{pmatrix} \begin{pmatrix} H \\ K \\ L \end{pmatrix}_{\text{fcc}} \tag{2}$$

and

$$\begin{pmatrix} H \\ K \\ L \end{pmatrix}_{\text{fcc}} = \frac{1}{27} \begin{pmatrix} 5 & -27 & -1 \\ 5 & 27 & -1 \\ 2 & 0 & 5 \end{pmatrix} \begin{pmatrix} h \\ k \\ l \end{pmatrix}_{(115)}, \tag{3}$$

with lattice parameters $a=13.281$ Å , $b=2.556$ Å , and $c=18.783$ Å . Thus the $(111)_{\text{fcc}}$ bulk Bragg peak is now indexed as $(603)_{115}$, as shown in the reciprocal-space map of Fig. 4. Bragg peaks are separated in l by 27 reciprocal-lattice units. That is, there are other Bragg peaks at $(6,0,30)_{115}$ and $(6,0,\overline{24})_{115}$, although these peaks are far beyond the q range accessible by this experiment. On the other hand, the interlayer spacing is deceptively small: $d_{\text{bulk}}=0.696$ Å, since there are 27 layers of atoms per unit cell. Atoms in adjoining planes have, of course, significant lateral separation, as seen in Fig. 3.

For vicinal surfaces, it is more natural to describe vertical displacements in terms of interatomic separation (projected onto the z axis) than to speak of interlayer spacings. For atoms in adjacent ''layers'' which have horizontal separations much larger than their vertical separations, the concept of interlayer spacing is less meaningful. The *change* in relative vertical position of an atom in layer i compared with an atom in layer $i+1$ can be defined as

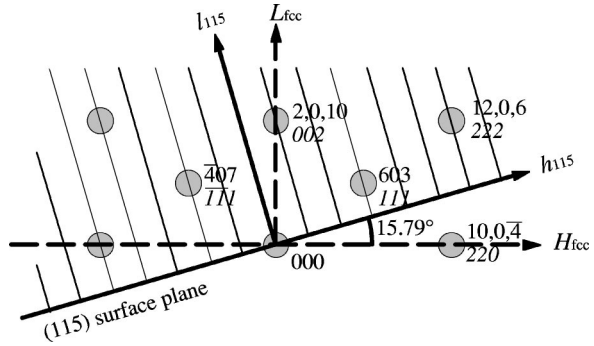

FIG. 4. Reciprocal space map for a fcc(115) surface, in the $k=0$ plane. Shaded circles represent Bragg points, labeled in standard fcc units (lower, italics) and 115 surface units (upper, straight). Axes for standard fcc orientation (dashed) and for 115 surface orientation (solid) are in bold. The narrow, tilted lines represent 115 crystal truncation rods. Note that this figure is rotated from Fig. 3.

$$\frac{\Delta z_i}{z_0} = \frac{\delta d_{i,i+1}}{d_{\text{bulk}}} = \frac{(z_i - z_{i+1}) - z_0}{z_0}. \tag{4}$$

z_i is the vertical position of the atom in the coordinates of the surface unit cell, and, for the Cu(115) surface unit cell, the bulk interlayer spacing $z_0=\frac{1}{27}$. Use of Δz_i instead of $\delta d_{i,i+1}$ emphasizes that atoms on vicinal surfaces may not be directly above the atom in the next layer down.

A. Previous work on Cu(115)

Work on the clean Cu(115) surface originally focused on the stability of this stepped surface, rather than the crystallographic structure. Time-of-flight helium atom scattering in Ref. 33 determined that this surface does *not* undergo a roughening transition, as previously thought. Energy analysis was essential to this experiment, given the large amount of inelastic scattering from this surface at high temperatures.

Low-energy electron diffraction (LEED) has been performed on Cu(115), and is interpreted as a complex multilayer relaxation.[34] The measured relaxation between the first and second lattice planes is $\Delta z_1/z_0=-13.2\%$, and relaxations continued to the sixth layer. Table I lists the results of this experiment. Although the fractional change $\Delta z_1/z_0$ is very large, the actual atomic displacement is not so dramatic since, as mentioned above, d_{bulk} is relatively small.

This LEED analysis considered only vertical displacements in the atomic relaxations, but a full crystallographic analysis should allow lateral displacements as well. Since no reconstruction was observed in either in-plane direction, we expect on symmetry grounds that atoms remain at $y=0$ or $\frac{1}{2}$ (gray or black circles in Fig. 3). The lack of mirror symmetry in the x direction allows, in general, for atoms to relax in this direction. LEED is typically more sensitive to interlayer displacements and surface x-ray diffraction to lateral displacements, so perhaps the LEED data could be sufficiently fit without including lateral displacements in the surface model.

The structure of Cu(115) was studied theoretically by Loisel *et al.*[35] using tight-binding calculations, by Ham-

TABLE I. Interlayer relaxations of Cu(115) as determined by LEED experiments (Ref. 34), tight-binding calculations (Ref. 35), energy-minimization calculations (Ref. 36), embedded-atom calculations (Ref. 37), and surface x-ray diffraction (present work). Reference 37 and the present work also explicitly include lateral displacements.

	Percent relaxation ($\Delta z_i/z_0$), determined by:				
Layer	LEED (Ref. 34)	tight-binding calculations (Ref. 35)	energy minimization calculations (Ref. 36)	embedded atom calculations (Ref. 37)	surface x-ray diffraction
1	−13.2	−8.0	−12.7	−9.46	−15.4
2	−6.1	−5.1	−10.3	−7.87	+8.1
3	+5.2	+7.0	+10.8	+8.76	−1.1
4	−0.1	−3.3	−6.3	−4.19	−10.3
5	+2.7	−3.1		−4.04	+5.4
6				+3.44	−0.7
7				−1.67	−6.9
8				−1.14	+3.6

monds and Lynden-Bell[36] using energy minimization calculations, and by Tian and Rahman[32] and Durukanoglu, Kara, and Rahman[37] using the embedded-atom method. All methods found a qualitatively similar relaxation pattern in the interlayer spacing, with $\Delta z_1/z_0$ not as extreme as determined by LEED;[34] results are shown in Table I. More recent embedded atom calculations[38] are in very good agreement with Refs. 32 and 37. Furthermore, Rahman and co-workers[32,37] found a common characteristic in several Cu(001) vicinal surfaces: the vertical displacements of subsurface (bulklike) atoms follow the trend set by atoms of the topmost layer. The displacement of the surface atoms are repeated inwards with an exponentially decaying scale factor. Multilayer relaxations of this sort are common in surface structure, but vicinal surfaces present a complication: for Cu(115), each atom is almost vertically aligned with the atom of the *third* layer below it (besides an offset of $\frac{1}{2}$ in y). Tian and Rahman[32] used the vertical displacements of the top atoms, Δz_m (where $m=S$, T, or C, the three surface sites defined in Fig. 3) to describe the displacements of the lower atoms:

$$\Delta z_{m,n}=\Delta z_m \exp[-\kappa_m(n-1)]. \quad (5)$$

n is the depth of the atom beneath the surface (Fig. 3), and κ_m is an exponential decay factor. The form of Eq. (5) is the general solution of the Poisson equation, which will be the exact solution in the limit of continuum elasticity theory. Although Ref. 32 did not consider lateral displacements, Ref. 37 did, finding that the trend of Eq. (5) approximately holds. The small displacements in x did not follow any such trend.

Durukanoglu, Kara, and Rahman[37] also calculated the surface phonon spectrum of Cu(115) and similar Cu(001) vicinal surfaces, finding highly anisotropic thermal vibrations at the surface. The in-plane phonon modes perpendicular to the steps were particularly softened, resulting in a large Debye-Waller factor in x for the step atoms (symbol B_x^S; the subscript represents direction and the superscript identifies the atom). Calculated vibrational amplitudes in x for terrace and corner atoms were progressively smaller, reflecting their greater coordination. Vibrational amplitudes in y were nearly identical for the S, T, and C atoms, and in z the trend was reversed from x, with the corner atoms having the largest mean-square amplitude. These results appear consistent with He-atom scattering experiments[39] which mapped out the surface-phonon-dispersion curves of Cu(115) and found a low-energy longitudinal mode at the zone boundary.

B. Present experiment and results

In order to determine the surface structure of Cu(115), we have performed a surface x-ray diffraction experiment at beamline X16A of the National Synchrotron Light Source, Brookhaven National Lab. The surface was prepared by chemical polishing, then by cycles of sputtering with 1-keV Ar^+ ions and annealing to 550 °C, until terraces on the surface were $\gtrsim$700 Å, as determined by the width of the crystal truncation rods. The structure factors (F_{hkl}), derived from integrated intensities of diffractometer ϕ scans, were corrected for Lorentz and polarization factors and the variation of the illuminated area on the surface. 123 structure factors along five crystal truncation rods[30] were measured at room temperature using 8.5-keV x rays. Structure factors for negative l are achieved through inversion symmetry using the Friedel relation $F_{hkl}=F_{\overline{hkl}}$, and crystallographically equivalent structure factors were symmetry averaged together using plane group pm: $F_{hkl}=F_{h\bar{k}l}$ due to mirror symmetry in y.

Figure 5 displays the structure factors measured from the Cu(115) surface. The dashed line represents the calculated scattering from a bulk-truncated Cu(115) surface; the only fitting parameters are an overall scale factor, a roughness parameter, and one isotropic Debye-Waller factor. The ideal bulk truncation made a reasonable preliminary fit, but the data had clear oscillations which called for a model with atomic displacements and additional Debye-Waller factors for the surface atoms. On this vicinal surface, the most general model has many atoms with independent displacement parameters, e.g., 14 free displacement parameters for the top seven layers of atoms (all of these atoms being close to the surface). Refining such a model produced a physically unreasonable fit: the distance from atom S (the step atom) to any of its nearest neighbors was greater than 2.6 Å, compared with the bulk bond length of 2.556 Å; the Debye-Waller factor for this atom also had a large, negative value (which has no physical meaning). Other interatomic distances on

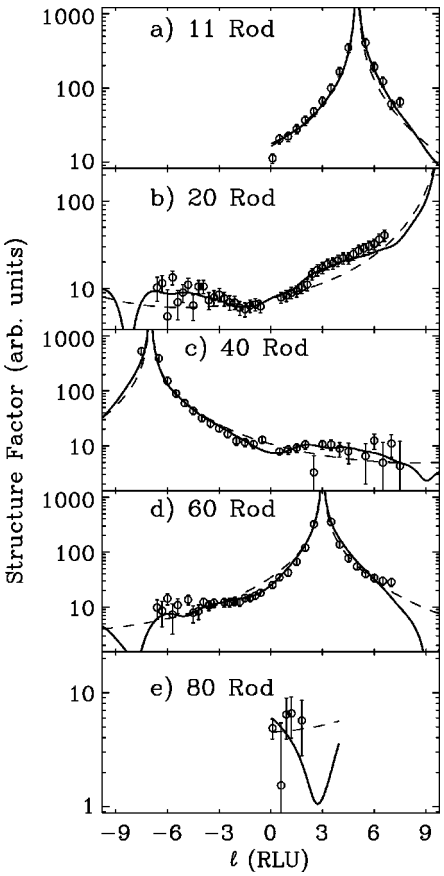

FIG. 5. Structure factors of the five crystal truncation rods of clean Cu(115). Circles represent data points, the dashed line is a fit for an abrupt bulk termination, without atomic displacements or multiple Debye-Waller factors ($\chi^2=2.47$); and the solid line is the best fit as described in the text ($\chi^2=1.40$). (a) $(11l)$ rod, whose bulk peak is at $l=5$. (b) $(20l)$ rod, whose bulk peak is at $l=10$. (c) $(40l)$ rod, whose bulk peak is at $l=-7$. (d) $(60l)$ rod, whose bulk peak is at $l=3$. (e) $(80l)$ rod, whose bulk peak is at $l=13$.

this surface became less than 2.2 Å . We conclude that this model provided too many degrees of freedom for the available data.

To attempt a more realistic description of the Cu(115) surface, we developed a model which included fewer free parameters combined with some physical insight. This model limited all vertical displacements to the form of Eq. (5). Thus an arbitrary number of atoms was allowed to relax in the z direction and be described by only four parameters: the z displacements of the step, terrace, and corner atoms (Δz_S, Δz_T, and Δz_C respectively) and one decay factor κ, using the definitions of Eq. (5).[32,37] In practice, we allowed vertical displacements to the 15th layer of atoms, and used one common κ instead of separate decay factors for the *S*, *T*, and *C* atomic columns.

In addition to these vertical displacements, displacements in x for the top four atoms and four Debye-Waller factors were needed to model the surface satisfactorily. The values of the refined parameters are listed in Table II, resulting in a fit to the data of $\chi^2=1.40$ and graphed as the solid line in Fig. 5. The simple constraint of Eq. (5) was apparently sufficient to constrain the model and still explain the observations. As expected, the step atom is significantly contracted

TABLE II. Refined parameters for the final model of Cu(115), as described in the text, yielding $\chi^2=1.40$. Structure factors calculated from this fit are the solid lines in Fig. 5. Δx_i is the displacement of atom i from its bulk-lattice-defined position in units of the surface unit cell. Δz_j is the vertical displacement of atom j from the atom at the next deepest site compared to the bulk displacement, as defined in Eq. (4).

Vertical displacements	Lateral displacements	Debye-Waller factors
$\Delta z_S/z_0=-0.154$	$\Delta x_S=-0.0009$	$B_x^{ST}=7.6$ Å^2
$\Delta z_T/z_0=+0.081$	$\Delta x_T=-0.0011$	$B_{yz}^{ST}=3.3$ Å^2
$\Delta z_C/z_0=-0.011$	$\Delta x_C=-0.0075$	$B^{C,S2}=1.9$ Å^2
($\kappa=0.4$)	$\Delta x_{S2}=0.0035$	$B^{\text{bulk}}=0.55$ Å^2

inward, towards its neighbors, in agreement with the LEED experiment.[34] The fit was not very sensitive to the decay parameter, so κ was fixed at 0.4, as suggested by the numerical calculations and simple force-constant model of Ref. 32.

As predicted by calculations of the phonon spectrum of the Cu(115) surface,[37] an anisotropic Debye-Waller factor for the surface atoms significantly improved the fitting. Instead of attempting a detailed comparison with the results of Ref. 37, we limited the number of Debye-Waller factors to the minimum needed to obtain a satisfactory fit. We found that four such parameters were sufficient: two anisotropic Debye-Waller factors (one for the x direction, and one for y and z) shared by atoms *S* and *T*; one isotropic factor shared by atoms *C* and *S*2; and a value of $B_{\text{bulk}}=0.55$ Å for all other atoms. Additional Debye-Waller parameters did not result in an improved fit.

In addition to the above parameters, our model included a roughness factor based on the geometrical model of roughness.[30] The best fit yielded $\beta=0.51$, a large value even for a metal. However, this, like the large values of $\Delta z_i/z_0$, was due to the very small interlayer spacing of this surface; the root-mean-square roughness was only 1.44 Å .

The low symmetry of this vicinal surface produced many atoms near the surface which had crystallographically independent x and z coordinates. Simply allowing these coordinates to vary independently did not produce a physically realistic fit, but a restricted model assuming elastic interactions did. One effect of including Eq. (5) is to limit unrealistic interatomic distances; most of the refined distances in the model ranged from 2.49 to 2.57 Å . Prevention of unrealistic interatomic distances can also be addressed by adding an ''energy cost'' to the goodness of fit parameter. That is, bond lengths (or also bond angles) far from bulk values add to the χ^2 of a model, ensuring a preference for realistic interatomic distances. This procedure has been employed[40] in the solving of complex reconstructions on semiconductor surfaces using the Keating model of interatomic potentials.[41] On the other hand, Eq. (5) is, to some extent, an oversimplification of the true multilayer displacements. Surface atoms will likely relax with some deviation from an exponential decay, which this model does not take into account. A more complete structure determination would require data from a greater range of reciprocal space, implying a higher x-ray energy. Unfortunately, more energetic x rays than those used in this experiment would cross the Cu *K* adsorption edge,

resulting in a high fluorescence background and making accurate integrated intensities more difficult to measure without an energy-sensitive detector.

III. STRUCTURE OF O/CU(104) FACETS

A. Previous work on O/Cu(104)

Unlike Cu(11n) surfaces, Cu(104) is a (001) vicinal surface with ⟨010⟩-type steps, i.e., $4(100)\times(010)$ in compact step notation.[31] The first four rows of atoms are all exposed to the surface (i.e., have reduced coordination); the steps are not close packed, resulting in a surface which is not expected to be thermodynamically stable.[42] Upon exposure to oxygen, however, this surface is known to become extremely stable.[43] The O/Cu(104) orientation is so strongly preferred that many nearby Cu(001) vicinal surfaces tend to form O/Cu(104) facets when exposed to O. Formation of O/Cu(104) facets has been observed by O dosing of many Cu surfaces, including Cu(115),[26] Cu(117),[24] Cu(1,1,11),[24] Cu(1,1,16),[23] Cu(102),[22] Cu(106),[27] Cu(108),[25,24] and Cu(418).[23] As mentioned above, other facets must also form in order to maintain, on average, the macroscopic orientation of the surface.

Due to the ⟨010⟩ orientation of the steps of the (104) surface, the lateral separation of Cu step atoms (along a step) is 3.61 Å. This exposes gaps along the step edges which provide an ideal adsorption site for O, since 1.85 Å ($\approx$3.61 Å /2) is the Cu-O bond length in Cu_2O and in several O-induced Cu reconstructions.[10] In fact, the O-Cu-O linear chains which form along these steps are often considered the stabilizing building block of the O/Cu(001)$(2\sqrt{2}\times\sqrt{2})$, O/Cu(110)$(2\times1)$, and O/Cu(110)$c$ (6×2) reconstructions.[10]

Despite the importance of the (104) surface in the O on Cu system, a full structural determination has not been performed, and studies to date remain ambiguous. Algra, Suurmeijer and Boers,[44] using low-energy ion scattering, found only one type of O adsorption site in Cu(104) for low O exposures, concluding that O_2 adsorbs dissociatively into the hollow sites of the steps. A photoelectron diffraction study by Thompson and Fadley[43] confirmed that O resides at the twofold step sites at low exposure, but at higher coverage also occupies a (001) terrace site, as proposed by Perdereau and Rhead.[21] More recently, Robinson, Vlieg, and Ferrer[9] hypothesized that O would sit in the hollow sites of the first and third Cu rows, and that the fourth Cu row would be missing; the (001) terraces on the vicinal surface then have a structure similar to the $2\sqrt{2}\times\sqrt{2}$ reconstruction of O/Cu(001). In the $2\sqrt{2}\times\sqrt{2}$ reconstruction, the O atoms are fourfold coordinated; if O atoms sit at the center of the first and third-row hollow sites of *unrelaxed* Cu(104), then the O atoms in the third row have five Cu neighbors *unless* the fourth Cu row is removed. Rutherford backscattering and channeling experiments[45,46] were not able to directly observe O on the Cu(104) surface, but did find a large outward expansion of the top atomic layers of $\sim$0.3 Å. A missing row was not needed to interpret this data, yet the data were consistent with the third or fourth row missing.

Several STM studies have examined the structure of O/Cu(104) facets formed by exposing various Cu(001) vicinal surfaces to O. Lloyd and Woodruff[25] initially labeled the O/Cu(104) facets of Cu(108) as missing the *second* Cu row, based on one low-resolution STM image. Knight, Driver, and Woodruff[27] reinterpreted that image as more likely missing the fourth row of Cu, consistent with their higher-quality images of O/Cu(104) formed by faceting of Cu(106). Reiter and Taglauer[26] interpreted their images of O/Cu(104) from the faceting of Cu(115) as missing the fourth Cu row.

B. Present experiment and results

In order to determine conclusively the surface structure of O/Cu(104), we have performed surface x-ray diffraction on the (104) [and equivalent (014)] facets. The faceted surface was prepared by exposing the clean Cu(115) surface (prepared as described in Sec. II B) to $\sim$50-L O_2 at 308 °C. Faceting was observed with the x rays, as described in Ref. 28, until (104), (014), and (113) facets had formed.

For this preparation, the coherence length in x (perpendicular to the steps) on the (104) facets was approximately 400 Å, as judged by CTR half-widths; in y, the coherence length was approximately 700 Å. These lengths on the (113) facets were approximately 300 Å in x by 1000 Å in y. These dimensions varied with preparation conditions (i. e., temperature, O_2 partial pressure, total O_2 dose). All structure factor measurements were performed after O dosing had ended and the sample had been cooled to room temperature.

The crystal truncation rods arising from these facets were no longer perpendicular to the Cu(115) surface, but instead each set of rods were perpendicular to the facet plane from which they arose, as shown in Fig. 1. The (104) and (014) CTR's are not parallel to the plane of Fig. 4; the (113) CTR's are in this plane, but are tilted 25.2° from [001]. To index these rods, we switched from (115) surface notation to the notation of the particular facet. Operationally, this was very easy to achieve by appropriately relabeling all of the alignment reflections in the diffractometer's orientation matrix. The reciprocal-space transformation from standard fcc units to the (104) surface units is given by

$$\begin{pmatrix} h \\ k \\ l \end{pmatrix}_{(104)} = \begin{pmatrix} 4 & 0 & 1 \\ 0 & 1 & 0 \\ -1 & 0 & 4 \end{pmatrix} \begin{pmatrix} H \\ K \\ L \end{pmatrix}_{\mathrm{fcc}}, \tag{6}$$

or, inversely,

$$\begin{pmatrix} H \\ K \\ L \end{pmatrix}_{\mathrm{fcc}} = \frac{1}{17} \begin{pmatrix} 4 & 0 & -1 \\ 0 & 17 & 0 \\ 1 & 0 & 4 \end{pmatrix} \begin{pmatrix} h \\ k \\ l \end{pmatrix}_{(104)}. \tag{7}$$

With this transformation, $(111)_{\mathrm{fcc}}=(603)_{115}=(401)_{104}$. Bulk peaks for the (104) surface are separated in l by 17 reciprocal-lattice units, and are connected by CTR's perpendicular to the (104) surface. In this tetragonal unit cell, $a=c=14.90$ Å and $b=3.615$ Å .

Since the average surface orientation, across many facets, is still (115), $l=0$ no longer represents the plane of grazing incidence or exit for the x rays relative to the (104) planes. For some rods, measurements can be made with the grazing incidence geometry for $l<0$. In other cases, $l\sim0$ is inaccessible. But for most of the $l<0$ measurements in Fig. 6, we use the inversion symmetry $|F_{hkl}|=|F_{\overline{hkl}}|$.

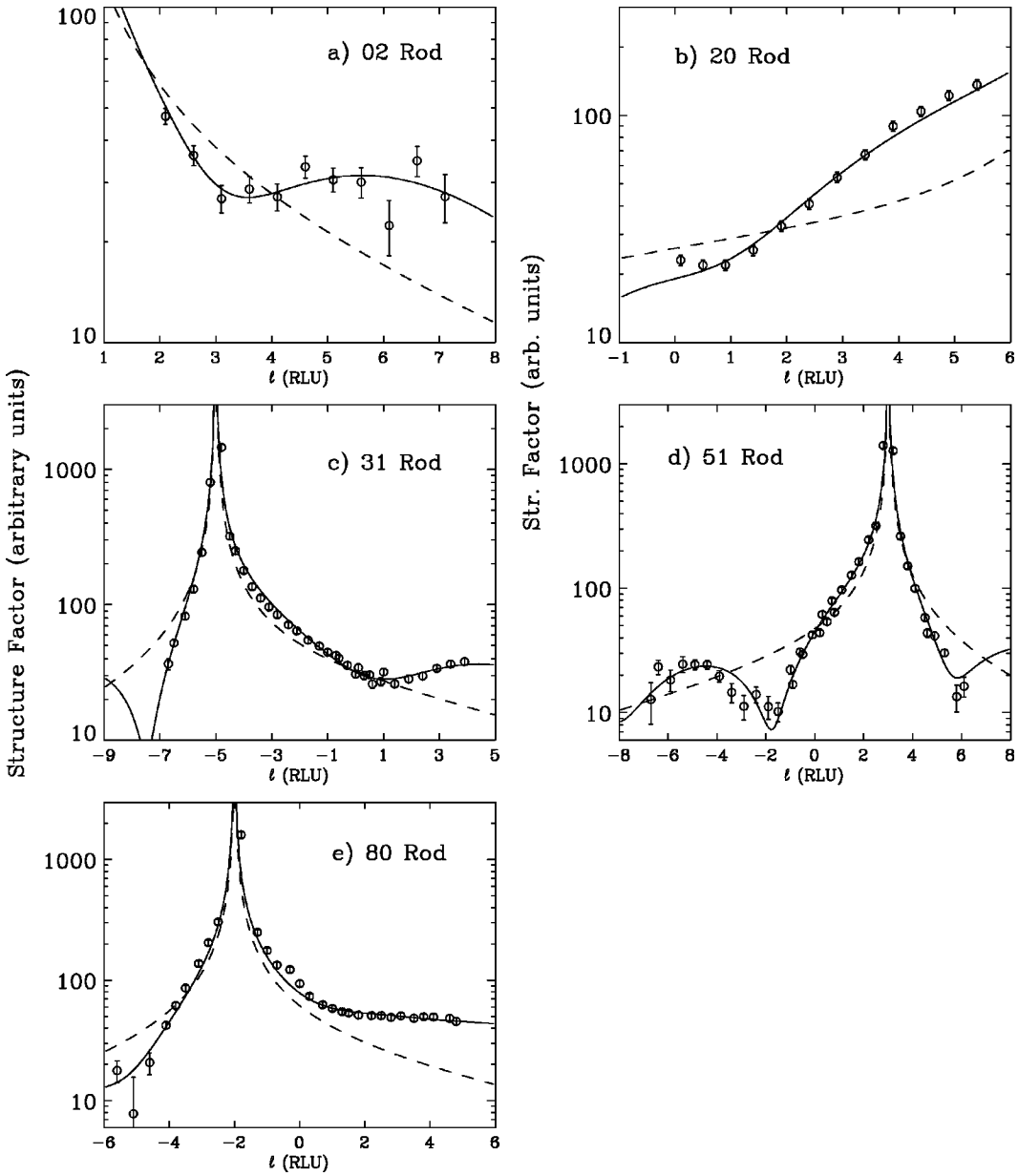

FIG. 6. Structure factors of the five CTR's of O/Cu(104) facets. Circles represent data points; the dashed line is a fit for an abrupt bulk termination, without atomic displacements or multiple Debye-Waller factors ($\chi^2=37.3$); and the solid line is the best fit as described in the text ($\chi^2=5.5$). (a) (02l) rod, whose bulk peak is at $l=0$. (b) (20l) rod, whose bulk peak is at $l=8$. (c) (31l) rod, whose bulk peak is at $l=-5$. (d) (51l) rod, whose bulk peak is at $l=3$. (e) (80l) rod, whose bulk peak is at $l=-2$.

Along with structure factors from O/Cu(104), we measured the structure factors from the crystallographically equivalent O/Cu(014) facets, finding, as expected, that data from both facets agreed well. Therefore, to achieve a better data set we averaged the measurements from the two facets together, along with the symmetry equivalents from each facet. In all, we measured 319 structure factors using 7.9-keV x rays, which symmetry average to 127 data points (the average agreement is 5.2%) along the five inequivalent rods shown in Fig. 6.

The structure factors along each truncation rod are strongly modulated, indicating a drastic modification of the surface structure away from a simple bulk truncation (represented as dashed lines in Fig. 6). Although the oscillations may be suggestive of a missing row, no such structure could be found that simultaneously fits the oscillations on all five rods. Instead, our best fit to the data is a model with *all rows present*, and O atoms in the hollow sites of the first row (step edge) and third row (terrace). The displacements of the atoms in the first five rows are listed in Table III, with calculated structure factors displayed as solid lines in Fig. 6. Excluding the O atoms from the model, while refining the same number of Cu displacements, results in a χ^2 value more than double that of our best model.

In our model of the surface, the first three rows of atoms relax upwards, away from the bulk. The average spacing between atoms in the top three rows and atoms in lower layers increases by $\sim 9\%$, fully consistent with ion channeling studies.[46] With the first three rows expanding away from the bulk, the comparison with the O/Cu(001)$(2\sqrt{2}\times\sqrt{2})$ superstructure[9,26] remains partially valid, even without the fourth row absent. Apparently, the expansion of the first

TABLE III. Refined parameters for the O/Cu(104) surface structure, resulting in $\chi^2=5.5$. Displacements are in fractions of the surface unit cell. For Cu atoms, displacements are relative to bulk-inferred positions. Displacements for O atoms are relative to the Cu atoms of the same layer (besides the displacement of $\frac{1}{2}$ in y). Uncertainties for Cu atom displacements are $\sim 2\times10^{-3}$ for Δz_i, $\sim 1\times10^{-3}$ for Δx_i, and about twice that for O atoms.

Atom	Layer i	Δz_i	Δx_i	Debye-Waller factors
O	1	+0.028	−0.003	~0
O	3	+0.015	+0.016	~0
Cu	1	+0.025	−0.0157	1.8 Å^2
Cu	2	+0.019	+0.0125	1.8 Å^2
Cu	3	+0.023	+0.0022	1.8 Å^2
Cu	4	–	+0.0046	0.55 Å^2
Cu	5	–	+0.0036	0.55 Å^2

three rows carries a lower energy cost than removing the fourth row. A side view of the relaxed structure is shown in Fig. 7.

One notable result of this analysis is that the facets are, within error, completely smooth: $\sqrt{\sigma^2}=0\pm0.1$ Å, as might be expected from the stability of the O/Cu(104) facets. That is, on the length scale of the facets, the steps on the surface are straight (unkinked) and unbunched, in agreement with the micrographs of Reiter and Taglauer.[26] Besides a Debye-Waller factor for the bulk Cu atoms of $B_{\rm bulk}=0.55$ Å^2, the Cu atoms of the first three rows had a separate factor, $B_{\rm surface}=1.8\pm0.2$ Å^2. The refined Debye-Waller factor of the O atoms was zero within error bars. In all, four displacement parameters were used for O atoms and eight for Cu atoms. Due to the fewer electrons in O than in Cu and the correspondingly smaller form factor, the positions of the O atoms are determined with slightly lower certainty than the Cu positions. Despite this model's excellent ability to reproduce the modulations of the structure factor along all five rods, the goodness-of-fit parameter is relatively large: $\chi^2=5.5$. We feel this is due not to any deficiency in the model, but to an underestimation of the systematic errors associated with the highly reproducible data. The χ^2 test weights each data point with the inverse square of the error, yielding a high goodness-of-fit measure even for good fits to data with small uncertainties.

We do find one striking dissimilarity with the O/Cu(001)$(2\sqrt{2}\times\sqrt{2})$ structure, in that the two O sites (in the first and third rows) are inequivalent. The O in the third row (terrace site) is fourfold coordinated with bonds ~1.84 Å to the Cu atoms in the second, third, and fourth rows; this is almost a planar structure quite unlike the O coordination on the $2\sqrt{2}\times\sqrt{2}$ structure or in bulk Cu_2O. The O in the first row (step-edge site) is only twofold coordinated; it is located

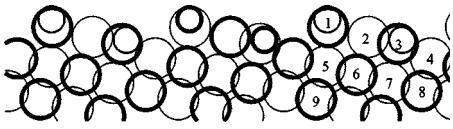

FIG. 7. Side view of refined O/Cu(104) surface structure. Bolder atoms are in the $y=0$ plane, while the lighter atoms are in the $y=\frac{1}{2}$ plane. O atoms have a smaller diameter than the Cu atoms.

TABLE IV. O-Cu bond lengths for the two O adsorption sites on Cu(104), with uncertainties of about 0.04 Å, based on refined atomic coordinates (Table III). In contrast, if the surface Cu atoms were unrelaxed and the O atoms were centered in the hollow spot of the step or terrace, then $d_{\text{O-}Cu}$ would be 1.807 Å for each bond length in the table.

O-atom site	Cu location	$d_{\text{O-}Cu}$ (Å)	Coordination
step (row 1)	row 1	1.855	2
	row 2	2.410	1
	row 5	2.540	1
terrace (row 3)	row 2	1.847	1
	row 3	1.837	2
	row 4	1.842	1
	row 6	2.420	1

1.85 Å from the adjoining Cu step atoms, but then >2.4 Å from the next nearest Cu atoms. Cu-O chains, without the fourfold coordination of O, are thus the main feature at this O site. Table IV details the nearest-neighbor Cu-O bond lengths resulting from our fit. This strong asymmetry in binding sites is not too surprising; on this stepped, vicinal surface, the O adsorption sites should not be degenerate as are the sites on the symmetrical $2\sqrt{2}\times\sqrt{2}$ surface. The steps on this vicinal surface produce the asymmetry in O adsorption sites observed in this work and previous studies.[44,43] We expect this asymmetry, not present on ideal (non-miscut) O/Cu(001)$(2\sqrt{2}\times\sqrt{2})$, significantly affects any rehybridization of Cu-O bonds.[47] This should be apparent in valence-band spectroscopy and in any future theoretical calculations which compare the total energies of the various O/Cu(104) surface structure models.

IV. STRUCTURE OF O/Cu(113)(3×1) FACETS

A. Previous work on O/Cu(113)

In contrast with the heavily studied O/Cu(104) system, very little work has been published regarding O/Cu(113), and most of that has concentrated on the (113) facets produced by exposing Cu(115) to oxygen. STM images by Reiter and Taglauer[26] show a moderately disordered structure on the (113) facets, with stripes about two atoms wide running parallel to the y direction. These stripes appear to be separated by about four monatomic Cu(113) steps; however, variations in stripe width and separation are clearly visible across the larger area scans. Along a stripe, atoms appear to be grouped in ''blocks'' about three atoms long, with gaps between the blocks about 1.6 Å wide. Occasional bright spots on the blocks were interpreted as ''superatoms'' elevated ~0.8 Å above the other atoms in the block. Based on the separation of stripes, length of blocks, and relative positions of neighboring ''superatoms,'' Reiter and Taglauer described this surface as a $c(12\times7)$ reconstruction.

Milne[48] also observed the formation of (113) facets due to O adsorption on two vicinal Cu surfaces. Electron microscopy indicated that O adsorption caused Cu(315) to form (305) and (113) facets, and reflection high-energy electron diffraction determined that O caused Cu(112) to facet to (223) and (113) orientations.[48] No structure was proposed for

these facets, and as they appeared only occasionally, they were likely metastable. During O_2 dosing on a single crystal Cu(113) surface, Fu and Somorjai[49] observed a $p(2\times1)$ reconstruction for O coverages of 0.4–0.5 ML, which reduced to 1×1 at higher coverages. Two nondegenerate O adsorption sites were identified based on desorption asymmetries, but no structural study was performed.

B. Present experiment and results

The disordered nature of the O/Cu(113) facets precluded the possibility of a full crystallographic analysis, yet, as Fig. 2 clearly shows, (113) CTR's were present in our data; the surface was, to some degree, flat and ordered. Following the procedure of Sec. III B for the case of O/Cu(104), we measured structure factors along six CTR's, which symmetry averaged to four, including those shown in Figs. 8(a)–8(c). Furthermore, we found a 3×1 reconstruction, indicating an ordered superstructure in *x but not in y*. Figures 8(d)–8(f) plot structure factors along three fractional order rods, while the full set of in-plane ($|l|\lesssim1$), third-order structure factors are shown in Fig. 8(g). Care was taken during measurement to exclude contamination from third-order harmonics in the x-ray beam; such features were much narrower and more intense than the superstructure rods, and therefore straightforward to isolate. In all, 300 structure factors were measured, symmetry averaging to 218 inequivalent points with an average agreement of 5.9%. The conversions between standard fcc coordinates and (113) surface coordinates are given by the matrices

$$\begin{pmatrix} h \\ k \\ l \end{pmatrix}_{(113)} = \begin{pmatrix} \frac{3}{2} & \frac{3}{2} & 1 \\ -\frac{1}{2} & \frac{1}{2} & 0 \\ -1 & -1 & 3 \end{pmatrix} \begin{pmatrix} H \\ K \\ L \end{pmatrix}_{\text{fcc}} \tag{8}$$

and

$$\begin{pmatrix} H \\ K \\ L \end{pmatrix}_{\text{fcc}} = \frac{1}{11} \begin{pmatrix} 3 & -11 & -1 \\ 3 & 11 & -1 \\ 2 & 0 & 3 \end{pmatrix} \begin{pmatrix} h \\ k \\ l \end{pmatrix}_{(113)}, \tag{9}$$

with resulting lattice parameters $a=8.477$ Å, $b=2.556$ Å, and $c=11.989$ Å.

Since all third-order rods are present (not just $3h+k$ equal to an integer), the 3×1 reconstruction was noncentered. Thus each (bulklike) layer of the surface contained six symmetry-inequivalent atoms. The modulation of the fractional order rods in Figs. 8(d)–8(f) indicated multilayer relaxations were also important in the structure of this reconstruction. The refinement of this many atomic positions presents a daunting task even for a well-ordered surface; the disorder made a complete crystallographic description unfeasible.

While our model does not determine all atomic positions on this surface, it does succeed in describing some features of these facets. We indeed found that a model containing stripes of Cu atoms fit the data best, in agreement with the STM work.[26] However, the STM also showed the atoms in the stripes did not have well-defined *y* values. The complete absence of superstructure reflections in *k* agreed with our interpretation of the STM images, that the stripes had no long-range order in the *y* direction. Our model attempted to account for the disorder in *y* by performing an incoherent average (summing of intensities) over two model surfaces. In each surface, the atomic positions were identical except for three Cu atoms, which exchanged *y* values. That is, if for one model surface, one ''disordered'' atom was located at $(x,0,z)$ then, for the other, the atom was at $(x,\frac{1}{2},z)$. This model is an obviously limited attempt at treating the surface's disorder, and ignores the variations in stripe width observed by STM.[26] The significant disorder on this surface makes it unlikely that any ''superatoms'' would be at well-defined crystallographic sites; attempts to refine positions of additional atoms on top of the stripes were unsuccessful.

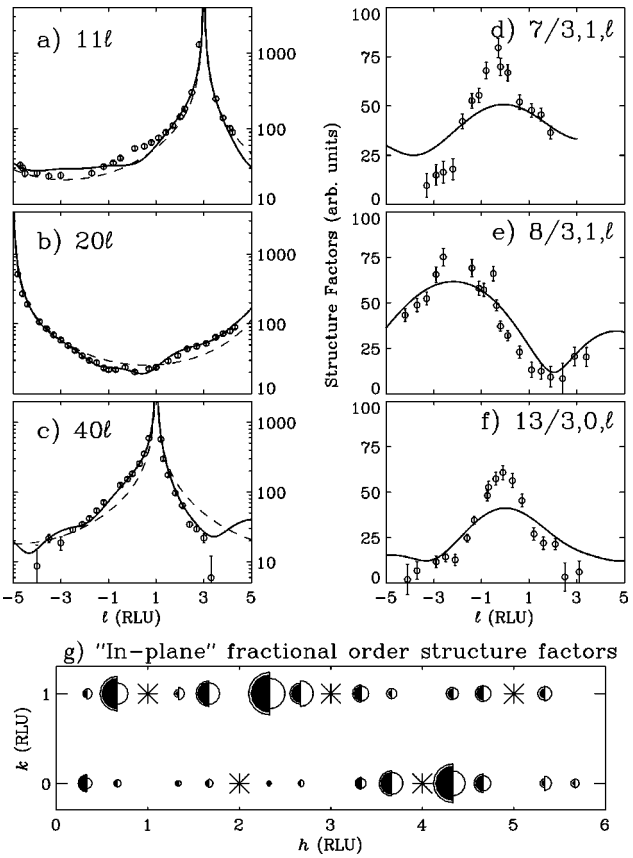

FIG. 8. Structure factors from rods of O/Cu(113) facets. Circles represent data points; dashed lines, the fit for an abrupt 1×1 bulk termination; and solid lines, the best fit as described in the text. (a)–(c) Structure factors from integer-order CTR's. Bulk peaks are located at (113), $(20\bar{5})$, and (401). (d)–(f) Structure factors from third-order rods. Note that the vertical axes of (a)–(c) are logarithmic, while those of (d)–(f) are linear. (g) Structure factors for in-plane third-order reflections ($|l|\lesssim1$). On the left are shaded semicircles whose radii are proportional to the measured structure factors, with the hollow, outer semicircles representing the error bars. On the right are values calculated from the best fit. Asterisks represent points where CTR's pass through the surface plane.

Like the O/Cu(104) facets, described in Sec. III B, which were smooth as measured by x rays, the O/Cu(113)(3×1) facets had $\beta=0\pm0.01$, using the geometrical model of roughness described in Ref. 30. One Debye-Waller factor of

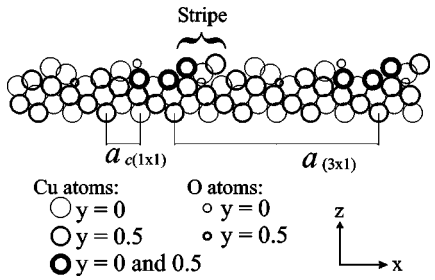

FIG. 9. Side view of the refined O/Cu(113)(3×1) surface structure. O atoms have a smaller diameter than Cu atoms. The thickness of the atoms shows whether they are located in the $y=0$ or $\frac{1}{2}$ plane, or both (to model the disorder on the surface). The bottom two rows of atoms are unrelaxed from their bulk positions.

$B=0.5$ Å^2 sufficed for all atoms; this model is not detailed enough for the relatively fine effects of additional Debye-Waller factors. Based on interatomic distances, three atoms per unit cell were tentatively identified as O, with the appropriate form factor used in calculation of the best fit. In the refinement of the atomic positions, 19 Cu atoms were allowed to relax from their bulk-defined positions, besides the three O atoms and the three Cu atoms ''disordered'' in y. Figure 9 is a side view of the refined positions of the atoms in our disordered stripe model. The structure factors calculated from this model are shown with the data in Figs. 8.

The goodness of fit parameter for the disordered stripe model is $\chi^2=7.9$; while certainly leaving room for improvement, this was the best achievable given the disorder on the surface. Most of the disagreement is associated with the third-order rod measurements rising and falling more abruptly than the model predicts. This is a symptom of an oversimplified model: deeper layer displacements are needed to increase the modulation, but would introduce many additional fitting parameters. It is not clear that such a procedure would produce reliable results. We expect our refined positions are the result of the ensemble average naturally performed by diffraction across many unit cells. Since the structure of the stripes is expected to vary in y [due to the blocks and possible ''superatoms'' observed with STM (Ref. 26)], the positions of the atoms beneath the stripes are also likely to vary with y. The results of the simple disordered stripe model picks out the laterally averaged position of each atom.

Applying surface x-ray diffraction to O/Cu(113) facets has helped elucidate the structure of these facets. Specifically, a noncentered 3×1 reconstruction was observed, and the measured data were most consistent with a disordered stripe model. However, the disordered nature of this surface precluded a full crystallographic analysis, therefore limiting the conclusions which could be drawn. For a more complete understanding of O/Cu(113), other surface science techniques, each with its own advantages and limitations, must be applied to this system.

V. CONCLUSION

In this paper we have presented three surface structure determinations, of a clean vicinal surface and of two oxygen-covered facets. While the determination of the O/Cu(104) facet structure demonstrates the power of surface x-ray diffraction to detect subsurface atoms, the determination of the Cu(115) surface structure and the O/Cu(113)(3×1) facet structure demonstrate the more common situation, of the need for multiple, complimentary surface science techniques (theoretical as well as experimental) to describe a surface fully. In the case of O/Cu(113)(3×1), additional work remains on both preparation and analysis of this disordered structure before a complete description can be reached.

We expect that our results for the O/Cu(104) facets should also describe the structure of bulk O/Cu(104) single-crystal surfaces. As discussed in Ref. 28, O/Cu(104) is one of the most stable O-covered Cu surfaces, and the formation of O/Cu(104) facets appears to drive the faceting of this system. It is conceivable that these facets may, in fact, be closer to the lowest-energy structure of O on Cu(104) than even O/Cu(104) from bulk single crystals. Bulk crystals may be hampered by misorientation, impurities, or incomplete O adsorption, while the facets are less susceptible to such limitations. In our preparation we are, in effect, growing the {104} substrate along with its surface.

In contrast, the (113) facets are formed primarily because the surface must maintain its macroscopic (115) orientation. These facets are significantly disordered and likely strained. Indeed, the reconstruction formed by O on a Cu(113) single crystal is supposedly quite different from the disordered stripes observed on the facets.[26,49] Nevertheless, now that several structures of O on Cu surfaces have been experimentally determined (and several other surfaces have been found to be unstable), the time is ripe for theoretical work to more completely describe the interactions of oxygen with both flat and stepped Cu surfaces.

ACKNOWLEDGMENTS

We would like to thank H. Meyerheim for use of the Cu(115) crystal, and E. Vlieg and D. P. Woodruff for helpful discussions. This research was supported by NSF Grant No. DMR 93-15691. The NSLS is supported by the U.S. Department of Energy under Grant No. DE-AC02-98CH10886.

*Present address: Department of Materials Science and Engineering, Northwestern University, 2225 North Campus Drive, Evanston, IL 60208.

[1] G. A. Somorjai and M. A. Van Hove, Prog. Surf. Sci. **30**, 201 (1989).
[2] T. N. Rhodin and G. Broden, Surf. Sci. **60**, 466 (1976).
[3] U. Bardi, Rep. Prog. Phys. **57**, 939 (1994).
[4] J. M. Carpinelli, H. W. Weitering, E. W. Plummer, and R. Stumpf, Science **381**, 398 (1996).
[5] H. Ibach, Surf. Sci. Rep. **29**, 193 (1997).
[6] F. Besenbacher and J. K. Nørskov, Prog. Surf. Sci. **44**, 5 (1993).
[7] R. Feidenhans'l, F. Grey, R. L. Johnson, S. Mochrie, J. Bohr, and M. Nielsen, Phys. Rev. B **41**, 5420 (1990).
[8] R. Feidenhans'l, F. Grey, M. Nielsen, F. Besenbacher, F. Jensen, E. Laegsgaard, I. Stensgaard, K. W. Jacobsen, J. K. Norskov, and R. L. Johnson, Phys. Rev. Lett. **65**, 2027 (1990).

[9] I. K. Robinson, E. Vlieg, and S. Ferrer, Phys. Rev. B **42**, 6954 (1990).
[10] W. Liu, K. C. Wong, H. C. Zeng, and K. A. R. Mitchell, Prog. Surf. Sci. **50**, 247 (1995).
[11] F. Jensen, F. Besenbacher, E. Lægsgaard, and I. Stensgaard, Surf. Sci. **259**, L774 (1991).
[12] F. Jensen, F. Besenbacher, and I. Stensgaard, Surf. Sci. **260/270**, 400 (1992).
[13] M. Polcik, J. Haase, M. Ondrejcek, and J. H. Petersen, Surf. Sci. **412/413**, 580 (1998).
[14] A. T. S. Wee, J. S. Foord, R. G. Egdell, and J. B. Pethica, Phys. Rev. B **58**, 7548 (1998).
[15] K. Morgenstern, H. Niehus, and G. Comsa, Surf. Sci. **338**, 1 (1995).
[16] Y. G. Shen, D. J. O'Connor, and K. Wandelt, Surf. Sci. **410**, 1 (1998).
[17] C. Ammer, K. Meinel, H. Wolter, and H. Neddermeyer, Surf. Sci. **401**, 138 (1998).
[18] G. Witte, J. Braun, D. Nowack, L. Bartels, B. Neu, and G. Meyer, Phys. Rev. B **58**, 13 224 (1998).
[19] W. Berndt, Z. Naturforsch. A **22a**, 1655 (1967).
[20] L. Trepte, C. Menzel-Kopp, and E. Menzel, Surf. Sci. **8**, 223 (1967).
[21] J. Perdereau and G. E. Rhead, Surf. Sci. **24**, 555 (1971).
[22] E. Legrand-Bonnyns and A. Ponslet, Surf. Sci. **53**, 675 (1975).
[23] J. C. Boulliard, C. Cohen, J. L. Domange, A. V. Drigo, A. L'Hoir, J. Moulin, and M. Sotto, Phys. Rev. B **30**, 2470 (1984).
[24] J. C. Boulliard, J. L. Domange, and M. Sotto, Surf. Sci. **165**, 434 (1986).
[25] G. W. Lloyd and D. P. Woodruff, Surf. Sci. **285**, L503 (1993).
[26] S. Reiter and E. Taglauer, Surf. Sci. **367**, 33 (1995).
[27] P. J. Knight, S. M. Driver, and D. P. Woodruff, J. Phys.: Condens. Matter **9**, 21 (1997).
[28] D. A. Walko, Ph.D. thesis, University of Illinois at Urbana-Champaign, 1999.
[29] D. A. Walko and I. K. Robinson (unpublished).
[30] I. K. Robinson, Phys. Rev. B **33**, 3830 (1986).
[31] B. Lang, R. W. Joyner, and G. A. Somorjai, Surf. Sci. **30**, 454 (1972).
[32] Z.-J. Tian and T. S. Rahman, Phys. Rev. B **47**, 9751 (1993).
[33] H.-J. Ernst, R. Folkerts, and L. Schwenger, Phys. Rev. B **52**, 8461 (1995).
[34] M. A. Albrecht, R. Blome, H. L. Meyerheim, W. Moritz, I. K. Robinson, and D. A. Walko (unpublished).
[35] B. Loisel, D. Gorse, V. Pontikis, and J. Lapujoulade, Surf. Sci. **221**, 365 (1989).
[36] K. D. Hammonds and R. M. Lynden-Bell, Surf. Sci. **278**, 437 (1992).
[37] S. Durukanoglu, A. Kara, and T. S. Rahman, Phys. Rev. B **55**, 13894 (1997).
[38] I. Y. Sklyadneva, G. G. Rusina, and E. V. Chulkov, Surf. Sci. **416**, 17 (1998).
[39] G. Witte, J. Braun, A. Lock, and J. P. Toennies, Phys. Rev. B **52**, 2165 (1995).
[40] J. S. Pedersen, Surf. Sci. **210**, 238 (1989).
[41] P. N. Keating, Phys. Rev. **145**, 637 (1966).
[42] S. Wei and M. Y. Chou, Phys. Rev. B **50**, 4859 (1994).
[43] K. A. Thompson and C. S. Fadley, Surf. Sci. **146**, 281 (1984).
[44] A. J. Algra, E. Suurmeijer, and A. L. Boers, Surf. Sci. **128**, 207 (1983).
[45] M. Sotto, Surf. Sci. **260**, 235 (1992).
[46] C. Cohen, A. L'Hoir, J. Moulin, D. Schmaus, M. Sotto, J.-L. Domange, and J.-C. Boulliard, Surf. Sci. **339**, 41 (1995).
[47] K. W. Jacobsen and J. K. Nørskov, Phys. Rev. Lett. **65**, 1788 (1990).
[48] R. H. Milne, Surf. Sci. **121**, 347 (1982).
[49] S. S. Fu and G. A. Somorjai, Surf. Sci. **262**, 68 (1992).